An eco-physiological model of forest photosynthesis and transpiration under combined nitrogen and water limitation

Peter Fransson[1,3], Hyungwoo Lim[1,2], Peng Zhao[1], Pantana Tor-ngern[4], Matthias Peichl[1], Hjalmar Laudon[1], Oskar Franklin[1,2]

[1]Department of Forest Ecology and Management, Swedish University of Agricultural Sciences, SE 901 83 Umeå, Sweden; [2]Ecosystems Services and Management Program, International Institute for Applied Systems Analysis, Laxenburg, A-2361 Austria; [3]Interdisciplinary Center for Scientific Computing, Heidelberg University, Heidelberg, D 69120 Germany; [4]Department of Environmental Science, Faculty of Science, Chulalongkorn University, 254 Payathai Rd, Wang Mai, Pathumwan, Bangkok 10330 Thailand

Author for correspondence:
Peter Fransson
Tel: +46732102241
Email: peter.fransson@iwr.uni-heidelberg.de

Keywords: Plant hydraulics, Stomatal model, Optimality theory, Nitrogen uptake, Scots pine.

Summary

- Forest growth is strongly affected by climate and soil conditions and reliable modelling these responses are needed to project forest growth for future climate scenarios. Although the separate effects of water and nitrogen limitations are well known, understanding how trees manage their combined requirements remains a challenge. Here we address this challenge based on a new eco-physiological model that accounts for plasticity in stomatal conductance and leaf nitrogen concentration.
- Based on an optimality principle, our model determines stomatal conductance and leaf nitrogen concentration by balancing C uptake maximization, hydraulic risk and cost of maintaining photosynthetic capacity.
- We demonstrate the accuracy of the model predictions compared to weekly GPP estimates from eddy flux measurements and canopy transpiration in long-term fertilized and unfertilized *Pinus sylvestris* forest in northern Sweden. The model also explains the response to increased soil N availability as a consequence of reduced carbon cost of N uptake and reduced hydraulic conductance per leaf area (linked to increased leaf area per sapwood area).
- The results suggest that leaves optimally coordinate N concentration and stomatal conductance both on short (weekly) time scales in response to weather conditions and on longer time scales in response to water and N availability in the soil.

Introduction

Human-made climate change has led to rising atmospheric CO_2 concentration, temperature rise and drought events (IPCC, 2014), which have major impacts on forest growth and gross primary production (GPP). On one hand one might expect that higher temperature can have positive effects on biomechanical processes of photosynthesis (Sage & Kubien, 2007) and hence growth. On the

other hand, more drought events increase the risk of hydraulic failure, and can even lead to mortality (Ryan, 2011). In addition, tree growth is limited by other factors, such as nitrogen (N) availability, which is particularly important in northern and boreal forests (Tamm, 1991; Binkley & Högberg, 2016). Thus, interactive effects of water and temperatures on photosynthesis and growth are further influenced by plant nutrition and soil N accessibility, yet such interactions are poorly incorporated in process-based models.

Process-based physiological models are well-suited for the task of assessing the response of photosynthesis to different climate drivers. One such model is the well-established Farquhar and von Caemmerer model of leaf photosynthesis (Farquhar *et al.*, 1980; Farquhar & von Caemmerer, 1982). To account for resource limitation of photosynthesis, this model can be complemented with models of stomatal conductance and photosynthetic capacity, which is linked to leaf N concentration. A number of semi-empirical models have been proposed to model the response of stomata, such as the Ball and Berry model (Ball *et al.*, 1987), where the stomatal conductance (g_s) is linearly related to the quantity AH_r/C_a. Here, A is the carbon assimilation rate, H_r is the relative humidity, and C_a is the ambient CO_2 concentration at the leaf surface.

One disadvantage of the empirical models is that they are parameterized based on a limited range of historical and experimental data, and thus may not be accurate under novel conditions or climate change. To overcome these limitations adaptive models based on optimization principles have been developed. These models assume that the responses of g_s and other traits to environmental fluctuation are regulated such that an optimal balance between maximizing carbon gain and minimizing cost is reached. In case of g_s, the apparent cost is the loss of water. Based on this premise Cowan & Farquhar (1977) proposed an optimization model where the carbon assimilation was set to A and the cost was assumed to be proportional to leaf transpiration, E, thus net gain = $A - E/\lambda$, where λ is a constant. While elegant, the assumption that the cost increases linearly with respect to E doesn't stand up to observations. Specifically, the cost increase should rise with respect to E, as a result of increased absolute water potential and thus bringing the vascular system closer to xylem cavitation. Mathematically, this means that the derivative of the cost function, with respect to E, should be an increasing function of E, which means that the cost function becomes concave-up (Wolf *et al.*, 2016). Eller et al. (2018) proposed the so-called SOX model in which the costs is a function of root–canopy hydraulic conductance, k_{rc}, to allow estimates of the response of tropical forest to drought and El Niño events. The underlying assumption is that the cost will increase as the k_{rc} decreases due to the increase in absolute water potential necessary to maintain E. While the above-mentioned models have only considered the cost associated with water transport, Prentice et al. (2014) proposed an alternative model in which the cost of maintaining photosynthetic capacity is incorporated into the cost term. The marginal cost of maintaining photosynthetic capacity was assumed to be proportional to $V_{\mathrm{c,max}}/A$, where $V_{\mathrm{c,max}}$ is the maximum rate of RuBP carboxylation. The drawback of the Prentice et al. (2014) model is similar to the Cowan & Farquhar (1977) approach, that the cost function, associated with transpiration, is not an increasing function of E. In contrast, a more recent approach by Joshi et al. (2022), called the P-hydro model optimize both photosynthetic capacity and has a transpiration cost increasing with E linked to increasing negative plant water potential.

In this study, we present a new leaf optimization model which combines the idea of accounting for the cost of maintaining photosynthetic capacity inspired by the P-hydro model (Joshi *et al.*, 2022) with the hydraulic cost representation of the SOX model. Thus, we optimize not only stomatal conductance as in the SOX model, but also the leaf N content. This leaf-based optimality model is upscaled to allow calculations of stand level GPP and canopy transpiration (E_c). We test and validate the model against observed GPP values derived from eddy flux measurements and E_c data for a *Pinus sylvestris* forest in northern Sweden, where 15 years of controlled annual fertilization has been

added alongside an untreated reference stand. This setting allows us to test our model with varying soil N availability and variable climate over several years. We show that the model predicts well the seasonal pattern of GPP and E_c. It also predicts the differences between control and N-fertilized plots as a consequence of different carbon costs of N uptake and leaf area per sapwood area.

Description

Model description

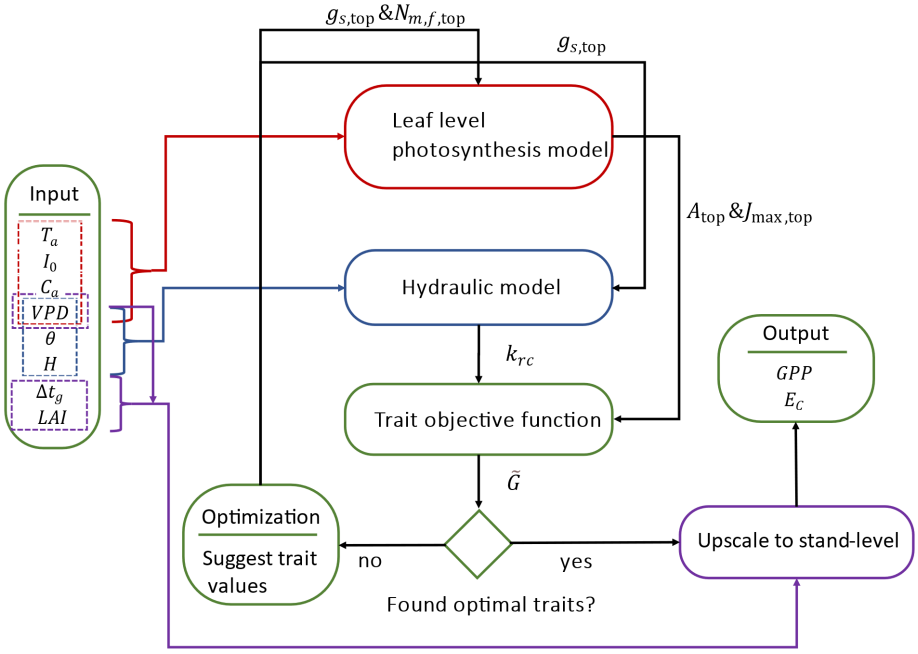

Fig. 1 The model is composed of four main modules: The leaf level photosynthesis model (LPM), The hydraulic model (HM), The trait objective function (TOF), and the upscaling module (UM). The modules are accompanied by an optimization routine (OR). To run the model, the following inputs are required: Mean ambient air temperature (T_a), above canopy photosynthetic active radiance (I_0), ambient carbon dioxide partial pressure (C_a), vapor pressure deficit (VPD), soil volumetric water content (θ), daylight hours (Δt_g), canopy height (H), and stand Leaf area index (LAI). OR is used to determine the value of the plastic traits, stomatal conductance ($g_{s,top}$) and mass-based foliage nitrogen concentration ($N_{m,f,top}$) of a leaf situated at the canopy top, by maximizing the trait performance measure ($\tilde{G}$). $\tilde{G}$ is determined by TOF with the root-canopy conductance (k_{rc}), carbon assimilation (A_{top}) and the potential rate of electron transport ($J_{max,top}$) as input. A_{top} and $J_{max,top}$ are calculated by LPM with T_a, I_0, C_a, VPD, $g_{s,top}$, $N_{m,f,top}$ as input. k_{rc} is calculated by HM with VPD, θ, H, and $g_{s,top}$ as in input. Once an optimum is found, UM upscales the leaf-level values to stand-level and we get the model output: per ground area canopy gross primary production (GPP), and canopy transpiration (E_C).

A flowchart of the model is provided in Fig. 1 and detailed descriptions of the sub-model are presented in the succeeding subsections. Our model predicts stand-level canopy gross primary production, GPP, canopy transpiration, E_c based on the LAI, stem density, canopy height, and climate data, see Table 1 for a full list of necessary inputs. We assume that physiological response is controlled by two plastic traits: the stomatal conductance (g_s) and foliage nitrogen mass-based concentration ($N_{m,f}$). More specifically, g_s and $N_{m,f}$ of a leaf/needle situated at the top of the canopy, denoted $g_{s,\mathrm{top}}$ and $N_{m,f,\mathrm{top}}$, respectively. The plastic traits are determined by optimization, maximizing the fitness proxy ($\tilde{G}$), which represents the net carbon gain per leaf area. $\tilde{G}$ is calculated as the leaf-level carbon assimilation of a leaf/needle situated at the top of the canopy (A_{top}) subtracted by the cost of maintaining transpiration and photosynthetic capacity, which depend on the function and costs of stem and roots supporting the leaf. Thus, $\tilde{G}$ can also be viewed as the

performance per leaf area and consequently we optimize on a leaf area basis. The cost of maintaining transpiration represents drought-related loss of root-canopy conductance (k_{rc}), e.g., due to xylem embolism, which corresponds to a proportional loss of supported leaf function (A_{top}). The cost of maintaining potential photosynthetic capacity (the potential electron transportation of a leaf situated at the canopy top, $J_{\text{max,top}}$ is due to respiration, which is proportional to leaf N content, and the carbon cost of N uptake, which depends on soil N availability. The calculation procedure of $\tilde{G}$ is as follows: First, A_{top} and $J_{\text{max,top}}$ are calculated using a mechanistic physiological model. A_{top} and $J_{\text{max,top}}$ are functions of climate variables (above canopy photosynthetic active radiation, I_0, ambient air temperature, T_a, ambient carbon dioxide partial pressure C_a, and vapor pressure deficit, VPD) and the two plastic traits. Next, k_{rc} is calculated by the hydraulic model with VPD, soil volumetric water content (θ), canopy height (H), and $g_{s,\text{top}}$ as input. Once the trait optimization routine finds the optimal trait values, GPP and E_c are calculated by upscaling the leaf-level values to the stand-level. Here, the stand leaf area index (LAI) and the daylight hours (Δt_g) are used as additional input.

Table 1. Model input. Value ranges are taken from weather data and modeled size data for the fertilized and control stand at Rosinedal experimental site (2015-2018). The data measurements are from 2015-2018, during the growth period.

Symbol	Description	Range (units)
		Climate and environmental input
T_a	Mean Ambient air temperature	3.5-21 (°C)
I_0	Above canopy photosynthetic active radiance	160.2-894.5 (µmol m^{-2} s^{-1}). These values are estimated from solar radiation data using the conversion rate 1000 W m^{-1} ≈ 2300 µmol m^{-2} s^{-1} (2.2.1.a,Landsberg & Sands, 2010)
C_a	Ambient carbon dioxide partial pressure	40 (Pa)
VPD	Vapor pressure deficit	50-1239 (Pa). Estimated from vapor pressure data and calculated saturated vapor pressure values. Saturated vapor pressure is calculated using eq 21 in Alduchov & Eskridge (1996)
θ	Soil volumetric water content	11.3- 27.2 (%) for the fertilized stand and 7.1- 19.1 (%) for the control stand
Δt_g	Daylight hours	10.6-20.3 (h). The daylight hours are calculated using eq 17 from Jenkins, (2013)
		Stand and tree size input
N	Stem density	847-850 (trees ha^{-1}) for fertilized stand and 1007-1010 (trees ha^{-1}) for control stand
H	Canopy height	19.07-19.87 (m) for the fertilized stand and 20.86-21.36 (m) for the control stand
LAI	Leaf area index (projected)	2.38-2.45 (m^2 m^{-2}) for the fertilized stand and 2.21-2.30 (m^2 m^{-2}) for the control stand

Leaf level photosynthesis model

The leaf level carbon assimilation is calculated in a standard fashion as a balance between the rate of assimilation (carbon demand) and the mass transport of carbon dioxide into the leaf through stomatal and mesophyll conductance (carbon supply). The assimilation rate, A, is calculated as the minimum of electron transport limited assimilation rate, A_j, and the carboxylation-limited assimilation rate, A_c, (Farquhar *et al.*, 1980). We assume co-limitation, i.e., that $A_c = A_j$ (coordination hypothesis, Chen et al., 1993). Further, we assume that the carbon assimilation rate $A = A_j$, thus,

$$\mathrm{A} = \frac{J}{4}\frac{c_i - \Gamma^*}{c_i + 2\Gamma^*}. \qquad \text{Eq. 1}$$

Here, c_i is he intercellular partial pressure of carbon dioxide, Γ^* is the carbon dioxide compensation point, and J is the rate of electron transportation, see Eq. 2.

$$J = \frac{\alpha I_\mathrm{I} + J_{max} - \sqrt{\alpha^2 {I_\mathrm{I}}^2 + 2\alpha I_\mathrm{I} J_{max}\left(1 - 2\theta_J\right) + J_{max}^2}}{2\theta_J}. \qquad \text{Eq. 2}$$

In Eq. 2 I_I is the irradiance incident on a leaf, J_{max} is the potential electron transportation, θ_J is a measure of the curvature of the light response curve, and α is the quantum yield. The mass transportation of carbon dioxide into the chloroplast through stomatal and mesophyll conductance is given by Fick's law:

$$A = g(c_\mathrm{a} - c_\mathrm{i}). \qquad \text{Eq. 3}$$

In Eq. 3 g is the combined stomatal (g_s) and mesophyll (g_m) conductance. We assume that g_m is proportional to g_s, thus $g \propto g_s$, specifically we assume $g \approx 0.42 g_s$ (Wang *et al.*, 2017). Because the demand and the supply equations need to be balanced, we get:

$$g(c_\mathrm{a} - c_\mathrm{i}) = \frac{J}{4}\frac{c_i - \Gamma^*}{c_i + 2\Gamma^*} \Leftrightarrow c_\mathrm{i}^2 + \left[\frac{J}{4g} + 2\Gamma^* - c_\mathrm{a}\right] c_\mathrm{i} - \left[\frac{J}{4g}\Gamma^* + 2c_\mathrm{a}\Gamma^*\right] = 0. \qquad \text{Eq. 4}$$

This is a quadratic equation and c_i is given by the greater of the two roots. Thus, we have an expression for c_i as a function of g, I_I, and J_{max}, i.e., $c_\mathrm{i}(g, I_\mathrm{I}, J_\mathrm{max})$. Similarly, we get an expression for the carbon assimilation by substituting Eq. 4 into Eq. 3,

$$A(g, I_\mathrm{I}, J_\mathrm{max}, c_\mathrm{a}) = g\left(c_\mathrm{a} - c_\mathrm{i}(g, I_\mathrm{I}, J_\mathrm{max})\right). \qquad \text{Eq. 5}$$

Temperature dependency of photosynthetic parameters and acclimation to annual temperature cycle

We use the Arrhenius equation and the model from (Tarvainen *et al.*, 2018) to estimate the short-term temperature dependency of the photosynthetic parameters. Specifically, the temperature responds of Γ^*, is modelled by using the Arrhenius equation (Landsberg & Sands, 2010),

$$\Gamma^* = \Gamma^*_\mathrm{ref}\ \exp\left(\frac{E_{A,\Gamma}(T - T_\mathrm{ref})}{TRT_\mathrm{ref}}\right),$$

where, $R = 8.314$ (J K^{-1} mol^{-1}) is the gas constant, $E_{A,\Gamma}$ is the activation energy of the parameter, T is the temperature (Kelvin), and Γ^*_ref is the parameter value at a reference temperature T_ref.
We use equation 4 from Tarvainen et al. (2018) to model the short-term temperature responds of J_{max},

$$J_\mathrm{max} = J_\mathrm{max,opt} f_\mathrm{Jmax}(T) = J_\mathrm{max,opt}\frac{E_{D,J}\exp\left(\frac{E_{A,J}\left(T - T_\mathrm{opt}\right)}{TRT_\mathrm{opt}}\right)}{E_{D,J} - E_{A,J}\left(1 - \exp\left(\frac{E_{D,J}\left(T - T_\mathrm{opt}\right)}{TRT_\mathrm{opt}}\right)\right)}.$$

Here, $E_{D,J}$ is the deactivation energy, $E_{A,J}$ is the activation energy, and $J_\mathrm{max,opt}$ is the value of J_max at optimal temperature T_opt (Kelvin).

On a longer timescale, parameters acclimate to the annual temperature cycle. Specifically, the magnitude of the light response curve (LSC) follows the trend of the temperature cycle while the shape of the curve remains constant (Hari & Mäkelä, 2003; Mäkelä *et al.*, 2004). Mäkelä et al. (2004) enforced this property by assuming that the quantum yield is proportional to J_{max}. For our model, we achieve the same effect by assuming that both J_{max} and the quantum yield, α, follow the same seasonal cycle, specifically, $\alpha = X_t \alpha_{\text{season}}$ and $J_{\max} = X_t J_{\max,\text{season}}(T_a, N_a)$. Here, α_{season} and $J_{\max,\text{season}}(T_a, N_{m,f})$ are parameters representing the seasonal apex of α and $J_{\max}$, respectively, and $X_t \in [0,1]$ is a variable accounting for the reduction of α and $J_{\max}$ due to the seasonal variation in temperature. Note that $J_{\max,\text{season}}(T_a, N_{m,f})$ depends on the ambient air temperature at, T_a, and the nitrogen concentration per leaf mass, $N_{m,f}$. If these equations are substituted into Eq. 2 we get,

$$J = \\ = X_t \frac{\alpha_{\text{season}} I_{\text{I}} + J_{\max,\text{s}}(T_a, N_{m,f}) - \sqrt{{\alpha_{\text{season}}}^2 {I_{\text{I}}}^2 + 2\alpha_{\text{season}} J_{\max,\text{s}}(T_a, N_{m,f}) I_{\text{I}}(1-2\theta) \ + J_{\max,\text{s}}\left(T_a, N_{m,f}\right)^2}}{2\theta}.$$

The time-dependent variable X_t is a function of the delayed ambient air temperature, S_t,

$$X_t = \begin{cases} 0, & S_t \le S_{\min}, \\ \dfrac{S_t - S_{\min}}{\Delta S}, & S_{\min} < S_t < S_{\min} + \Delta S, \\ 1, & S_t \ge S_{\min} + \Delta S, \end{cases}$$

where $S_{\min}$ is a parameter representing the minimum threshold for the activation of photosynthesis, and $\Delta S \ge 0$, is a parameter controlling when the photosynthetic capacity reaches its seasonal peak. Thus, $J_{\max}$ increases linearly with respect to S_t in the temperature range $S_{\min} < S_t < S_{\min} + \Delta S$. The delayed temperature, S_t, is modelled using a first order delay dynamics model (Mäkelä *et al.*, 2004, 2008),

$$S_t = \left(1 - \frac{1}{\tau}\right) S_{t-1} + \frac{1}{\tau} T_t, \qquad S_0 = T_0,$$

where T_t is the ambient air temperature at time t, T_0 is an initial temperature of a temperature time series, and τ is a parameter controlling the temperature delay; A higher value of τ equals a longer delay in the temperature response.

The effect of nitrogen concentration on the photosynthetic capacity

We assume that the seasonal apex of $J_{\max,\text{opt}}$ is proportional to the per leaf-mass nitrogen concentration, $N_{m,f}$, i.e., $J_{\max,\text{opt}}\left(N_{m,f}\right) = a_{Jmax} N_{m,f}$ (Franklin, 2007; Landsberg & Sands, 2010). Here, a_{Jmax} is a proportionality parameter. Thus, $J_{\max,\text{season}}\left(T_a, N_{m,f}\right) = J_{\max,\text{opt}}\left(N_{m,f}\right) f_{\text{Jmax}}(T_a)$ and $J_{max} = X_t J_{\max,\text{opt}}\left(N_{m,f}\right) f_{\text{Jmax}}(T_a)$.

Hydraulics model

If g_s and VPD, are given, we can calculate the canopy transpiration per leaf area, E, as,

$$E = \frac{1.6 g_s VPD}{P},$$

where P is the atmospheric pressure. We assume that the water flow between root and leaf is in steady-state and neglect non-stomatal water loss, thus E equals the water uptake. We use Darcy's law to calculate the canopy water potential, ψ_c, as a function of soil water potential, ψ_s, and E (Eller *et al.*, 2018),

$$\psi_c = \psi_s - H\rho g - \frac{E}{k_{rc}}. \qquad \text{Eq. 6}$$

Here, ρ = 997 kg m^{-3} is the density of water, g = 9.82 m s^{-2} is the gravitational acceleration, and k_{rc} is the root-canopy conductance. k_{rc} decreases from a potential maximal value, $k_{rc,\max}$, as water potential, ψ, declines according to the vulnerability function, $P(\psi)$,

$$P(\psi) = \frac{k_{rc}}{k_{rc,\max}} = \left(\frac{1}{2}\right)^{\left(\frac{\psi}{\psi_{50,rc}}\right)^{b_{rc}}},$$

where, $\psi_{50,rc}$ is the water potential resulting in half of the maximum conductivity, i.e., $P(\psi_{50,rc}) = 0.5$, and b_{rc} is a form parameter controlling how fast k_{rc} decreases with the water potential.
We calculate ψ_s from the effective soil saturation, S_e, by applying equation 2.19 from Jansson & Karlberg (2011),

$$\psi_s = \psi_a\, S_e^{-1/\lambda},$$

where, ψ_a is the air-entry tension and λ is the pore size distribution index of the soil.
The effective saturation is a function of soil water content (Jansson & Karlberg, 2011), θ,

$$S_e = \frac{\theta - \theta_r}{\theta_s - \theta_r},$$

where, θ_s is the saturated soil water content and θ_r is the residual water content.

We calculate k_{rc} by solving the equation (Sperry & Love, 2015),

$$k_{rc} = k_{rc,\max} \frac{\int_{\psi_c}^{\psi_{c,pd}} P(\psi)\, d\psi}{\psi_{c,pd} - \psi_c}, \qquad \text{Eq. 7}$$

where, $\psi_{c,pd} = \psi_s - H\rho g$ is the pre-dawn canopy water potential. See Methods S1 and Methods S2 for more information regarding how Eq. 7 is solve numerically.

Trait optimization

The plastic traits $N_{m,f,\text{top}}, g_{s,\text{top}}$ are determined through optimization of the trait performance measure, $\tilde{G}$,

$$N_{m,f,\text{top}}, g_{s,\text{top}} \coloneqq \operatorname{argmax} \tilde{G}.$$

We define $\tilde{G}$ as the carbon assimilation rate at canopy top, $A_{\text{top}} = A(g_{s,\text{top}}, I_{I_0}, J_{\max,\text{top}})$, reduced by potential conductance limitation , k_{cost} (Eller et al., 2018), and the cost of maintaining J_{max}, i.e. $N_s J_{max,top}$. Thus,

$$\tilde{G} = A_{\text{top}} k_{\text{cost}} - N_s J_{max,top}.$$

Here, k_{cost} is the ratio between the root-canopy conductance and the maximal conductance, i.e., $k_{\text{cost}} = k_{rc}/k_{rc,\max}$. For the $A_{\text{top}}(1 - k_{\text{cost}})$ cost term we assume that: 1) each fraction of k_{rc} corresponds to an equal loss in functional leaf area and thus assimilation loss and 2) in the event of hydraulic failure and fatal embolism, i.e., when k_{rc} decreases and approaches 0, the loss should be equal to the total carbon gain. N_s (unitless) is a site-specific cost parameter representing the carbon cost of constructing and maintaining photosynthetic capacity. These costs have two components: (i) maintenance respiration per $J_{\max}$, which is linked to leaf N because photosynthetic capacity and $J_{\max}$, increases with leaf N concentration associated with photosynthetic proteins and (ii) carbon investment (fine-roots, mycorrhiza, exudation) for the N uptake required per $J_{\max}$. Whereas maintenance respiration per $J_{\max}$ is an internal physiological process that should be constant among trees of the same species in the same climate, the cost for N uptake decline with increasing soil N availability. Thus, differences in the cost parameter N_s between our test stands reflects differences in soil N availability.

The trait optimization problem is solved by using the implementation of Broyden–Fletcher–Goldfarb–Shanno algorithm (BFGS) from the *Optim.jl* package (K Mogensen & N Riseth, 2018). We search the optimum in the range $0.007 \leq N_{m,f} \leq 0.05$ and $0.001 \leq g_s \leq \min(0.5, g_{s,crit})$. Here, $g_{s,crit}$ is the stomatal conductance which results in $P(\psi_c) = 0.12$, see *Methods S1*.

Upscaling to stand-level

Stand level primary production

We assume that $J_{\max}$ and g_s acclimate to irradiance resulting in a proportional relationship with irradiance level (Landsberg & Sands, 2010). Then the instantaneous gross primary production of canopy per ground area, GPP_c, is calculated as,

$$GPP_c = \int_0^{LAI} A(g_s, I_I, J_{\max}) dLAI = \frac{1 - \exp(-k \times LAI)}{k} A\left(g_{s,\mathrm{top}}, I_{I_0}, J_{\max,\mathrm{top}}\right).$$

Here, LAI is the leaf area index (projected area), and $g_{s,\mathrm{top}}, I_{I_0}$ and $J_{\max,\mathrm{top}}$ are the stomatal conductance, irradiance incident on a leaf, and $J_{\max}$, of foliage situated at the top of the canopy, respectively, see *Methods S3* for further details. The gross primary production of the canopy over a time-step, Δt, is approximated as $GPP_c \cdot \Delta t_g$. Here, Δt_g is the total daylight portion of Δt. In order to compare with measurements of whole forest stand fluxes, we have to account for understory vegetation GPP data, GPP_g, to calculate the ecosystem GPP, $GPP_e = GPP_c + GPP_g$. We assume that light use efficiency (LUE, defined as GPP/absorbed light) is the same for both vegetation layers (Tian *et al.*, 2021). GPP_c can then be upscaled by using an upscale factor, $\zeta = GPP_e/GPP_c$. The value of ζ depends on the understory vegetation LAI and corresponding light extinction coefficient, see *Methods S4* for more information. We estimate that $\zeta \approx 1.2$ for the fertilized stand and $\zeta \approx 1.13$ for the control (See Table S1). These corresponding contribution of GPP_g to GPP_e was 17% and 12% for the fertilized stand and control, respectively. This is in line with previous estimates (Chi *et al.*, 2021). Hereafter we will refer to GPP_e as simply GPP.

Canopy transpiration

We neglect the effects of boundary layer conductance (combined leaf and canopy boundary layer), thus the canopy transpiration E_c is calculated as,

$$E_c = g_C \frac{VPD}{P}.$$

Here, g_C is the canopy conductance. The canopy conductance is calculated as,

$$g_C = 1.6 \int_0^{LAI} g_s dLAI = 1.6 g_{s,\mathrm{top}} \frac{1 - \exp(-k \times LAI)}{k},$$

see *Methods S3* for further details.

Data

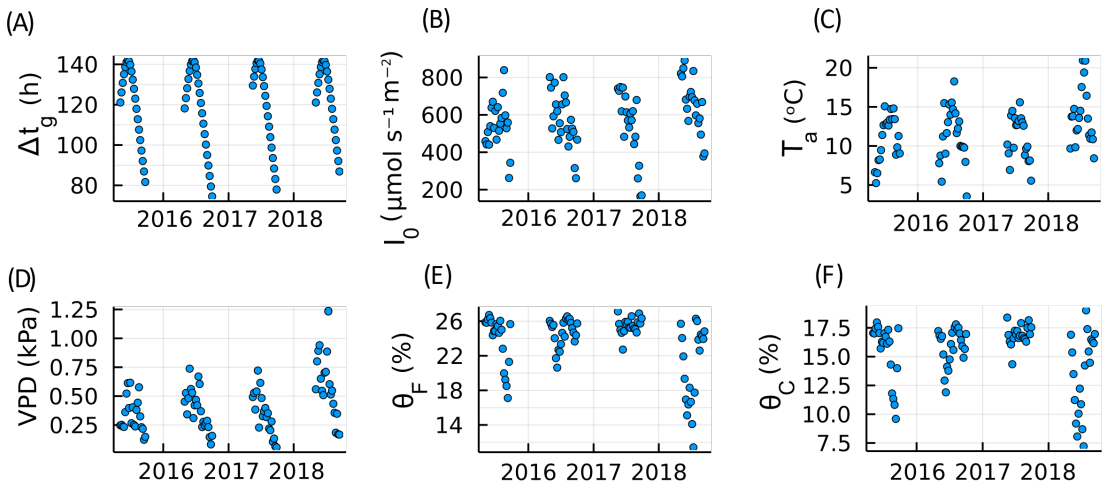

Fig. 2. Weather data for the fertilized and control stand at the experimental site Rosinedal during the growth period between 2015-2018. Climate drivers: daylight hours (Δt_g) (A), photosynthetic active radiance (I_0) (B), Mean daytime ambient air temperature (T_a) (C), vapor pressure deficit (VPD) (D), soil volumetric water content of the fertilized stand (θ_F) (C) and control stand (θ_C) (D). These were used as input for our model.

The data used for model calibration are based on measurements from the experimental site Rosinedal (64°10′ N, 19°45′ E). The site is a 90-year-old naturally regenerated *P. sylvestris* forest, regenerated with seed trees in 1920-1925. In 1955 the stand was pre-commercially thinned, followed by thinnings in 1976 and 1993. The experiment was established in 2005 and annual nitrogen fertilization started in 2006 with addition of 100 kg N ha^{-1} $year^{-1}$ from 2006 to 2011, and reduced to 50 kg N ha^{-1} $year^{-1}$ in 2012 (Lim *et al.*, 2015).We used weather data and measured tree dimensions from the fertilized and the control stand as input for the model, see Table 1 for a full list of input variables and Fig. 2 for a depiction of the weather data time series. Briefly, stem diameter was measured at 1.3 m (DBH) annually for all trees in each of the three mensuration plots (1000m^2) for each treatment stand. Tree height and length of live crown were measured on 20 trees per plot, using Vertex 4 Ultrasonic Hypsometer (Haglöf Inc., Sweden). We developed a relationship between height and DBH following the recommendation of Näslund (1947); parameters of the function were estimated in each year for each plot, and then applied to all individual trees. Biomass of each component and stem volume were predicted based on a combination of the tree dimensions and site-specific allometric equations, which were developed based on destructive tree harvesting in June 2006, October 2012, and October 2018. From 2012 and 2018 harvests, we scanned fresh foliage samples and dried to estimate specific leaf area. We then estimated leaf area index during the growing season by multiplying foliage biomass and specific leaf area estimates in addition of leaf litterfall during the growing season. Model outputs were calculated using weekly mean values (mean of daily values over a week) and validated against Eddy flux-based estimates of GPP (ecosystem) (Zhao *et al.*, 2022) and associated E_C values for the growth periods of 2015-2018. The growing season was assumed to start when daily mean temperature ≥ 5 °C for five successive days, and end when daily mean temperature was below 5 °C for five successive days. The E_C values are estimated using the empirical model from Tor-Ngern et al. (2017) with corresponding parameter estimates for the study site, provided in that paper. The validation data were converted to weekly mean values from daily data.

Parameter estimation

Table 2. Parameter values used in the model.

Parameter	Description	Value (units)	Reference/Note
	Gross primary production model parameters		
$\Gamma^*_{\mathrm{ref}}/E_{A,\Gamma}$	The CO_2 compensation point at 25 °C/Activation energy of Γ^*	4.17 (Pa)/ 23.42 (kJ mol^{-1})	Table 3.1 in Landsberg & Sands (2010)
$E_{A,J}/E_{D,J}/T_{\mathrm{opt}}$	Activation energy of $J_{\max}$/ Deactivation energy of $J_{\max}$/Optimal temperature for $J_{\max}$	47.4 (kJ mol^{-1}) / 200 (kJ mol^{-1}) / 305 (K)	(Tarvainen *et al.*, 2018)
θ_J	Curvature of the light response curve	0.7 (-)	Table 3.1 in Landsberg & Sands (2010)
k	light extinction coefficient	0.52 (-)	(Tian *et al.*, 2021)
m	Leaf transmittance	0.05 (-)	ch. 5.1.1 in Landsberg & Sands (2010)
	Hydraulics model parameters		
$\psi_{50,rc}/b_{rc}$	water potential which causes 50% loss in root-canopy hydraulic conductivity/Sensitivity of root-canopy hydraulic conductivity to water potential	-2 (MPa) / 2 (-)	
θ_s/θ_r	Saturated soil water content/ Residual water content	0.41 (-) / 0.006 (-)	From unpublished Pf-curve
ψ_a/λ	air-entry tension/pore size distribution index	-0.098 (MPa) / 1 (-)	From unpublished Pf-curve

Table 3. Estimated parameters. All parameters were shared among the stand treatments (fertilized F and control C), except when indicated by an asterisk (*).

Parameter	Description (units)	Estimates	
		F	C
	Nitrogen cost parameter		
N_s	Cost parameter of maintaining $J_{\max}$ (-)	0.023*	0.051*
	Gross primary production model parameters		
α_{season}	seasonal apex value of quantum yield peak (-)	0.14	0.14
a_{Jmax}	Ratio between $J_{\max,\mathrm{opt}}$ and Nitrogen concentration per leaf area ($N_{m,f}$) (mol m^{-2} s^{-1} kg leaf Kg^{-1} leaf N).	0.011	0.011
ΔS	Parameter controlling when the photosynthesis is at full capacity (°C)	17.29	17.29
τ	Parameter controlling the temperature delay (days)	14.45	14.45
	Hydraulics model parameters		
$k_{rc,\max}$	Maximum root-canopy hydraulic conductance (per leaf area) (mol m^{-2} leaf s^{-1} MPa^{-1})	0.00094*	0.0013*
	Variance parameters		
$a_{GPP,j}/b_{GPP,j}$	The parameters which control the variance of the error distribution for GPP (g C m^{-2} ground day^{-1}/-)	0.68/0.03	0.68/0.03

We estimated the unknown set of parameters of the model, $\boldsymbol{\theta}$ (see Table 3 for a full list of estimated parameters), by fitting the model to observations. The remaining model parameters were taken from other sources, see Table 2. To minimize the effect of data outliers, we assume that model and measurement errors are Laplace distributed (Tian *et al.*, 2021), i.e., $y_{i,j,k} - M\left(X_{j,k}, \boldsymbol{\theta}\right)_{i,j,k} =$

$e_{i,j,k} \sim Laplace\left(0, a_i + b_i M(\boldsymbol{\theta})_{i,j,k}\right)$. Here, $y_{i,j,k}$ denotes the response variables (the measured variables), $X_{j,k}$ are the collection of explanatory variables (tree size and climate data). M is the model output, $e_{i,j,k}$ are the model errors, $Laplace(\mu, b)$ is the Laplace distribution with location parameter μ and scale parameter $b > 0$. The parameters a_i and b_i control the variance of the error distribution and we assume that the scale parameter is linear with respect to the model output (Tian *et al.*, 2021). The subscripts i, j, k denotes the data type (GPP, E_C, or $N_{m,f}$), the stand treatment (control or fertilized), and the data index (individual observations), respectively. This assumption leads to the following likelihood function,

$$L(Y|\boldsymbol{\theta}, \boldsymbol{a}, \boldsymbol{b}) = \prod_i \prod_j \prod_k \frac{1}{2\left(a_{i,j} + b_{i,j} M(\boldsymbol{\theta})_{i,j,k}\right)} \exp\left(-\frac{|e_{i,j,k}|}{a_{i,j} + b_{i,j} M(\boldsymbol{\theta})_{i,j,k}}\right).$$

Here, $\boldsymbol{a}, \boldsymbol{b}$ are collections of a_i and b_i values, respectively.

The values for $y_{N_{m,f},j,k}$, $a_{N_{m,f},j}$, and $b_{N_{m,f},j}$ were estimated from data (Lim et al., 2015) ($y_{N_{m,f},\text{Fertilized},k} = 0.018$, for all k, $a_{N_{m,f},\text{Fertilized}} = 0$, $b_{N_{m,f},\text{Fertilized}} = 0.0018$ and $y_{N_{m,f},\text{Control},k} = 0.011$, for all k, $a_{N_{m,f},\text{Control}} = 0$, $b_{N_{m,f},\text{Control}} = 0.0018$), the values of $a_{E_c,j}$ and $b_{E_c,j}$ where taken from (Tian et al., 2021) ($a_{E_c,\text{Fertilized}} = 0.069$, $b_{E_c,\text{Fertilized}} = 0.15$ and $a_{E_c,\text{Control}} = 0.043$, $b_{E_c,\text{Control}} = 0.18$), while $a_{GPP,j}$ and $b_{GPP,j}$ were estimated in conjunction with the unknown model parameters.
The parameter estimates, $(\boldsymbol{\theta}^*, a_{GPP,j}{}^*, b_{GPP,j}{}^*)$, were determined by maximization of the likelihood function, i.e., $\boldsymbol{\theta}^*, a_{GPP,j}{}^*, b_{GPP,j}{}^* = \arg\max_{\boldsymbol{\theta},\boldsymbol{a},\boldsymbol{b}} L(Y|\boldsymbol{\theta}, a_{GPP,j}, b_{GPP,j})$. To find the maximum, we employed the adaptive differential evolution optimizer, a global optimization algorithm, from the *BlackBoxOptim.jl* package (Feldt, 2018).

We performed two parameter estimation and validation cases: One where all the parameters in Table 3 are shared between the two stand treatments, i.e., same parameter values were used for both treatments, with the exception of N_s and $k_{rc,\max}$. In a second case, none of the parameters in Table 3 were shared between the two stand treatments, i.e., the parameters were estimated separately for the control and fertilized stand. The result of the first case will be shown in the *Results* section and the result of the second case can be viewed in *Methods S5* and Fig. S3-Fig. S5.

Model validation

To validate our model, we excluded 20% of the datapoints (17 out of 84 datapoints) to form a validation dataset. The validation dataset was generated by randomly selecting datapoints from the complete dataset. The remaining datapoints, the training dataset, were used for parameter estimation. To minimize the effect of selection bias, we repeated the parameter estimation and validation process 10 times for both cases, thus creating 10 random validation and training datasets.

Results

The model can predict seasonal changes in GPP and E_C

The result for the parameter estimation is depicted in Fig. 3. Estimated parameters are provided in Table 3. The average R^2 for all datapoints (training set + validation set), i.e. the average R^2 over all 10 optimization runs (error estimates for all 10 runs are depicted in Fig. S2), was 0.60 (GPP) and 0.93 (E_C) for the fertilized stand. The corresponding values for the control were 0.71 (GPP) and 0.93 (E_C) (Table 4). Overall, our model was able to capture the inter-seasonal variation of GPP and E_c. The model slightly overestimates the GPP values for the fertilized stand and underestimated for the control (Fig. S1).

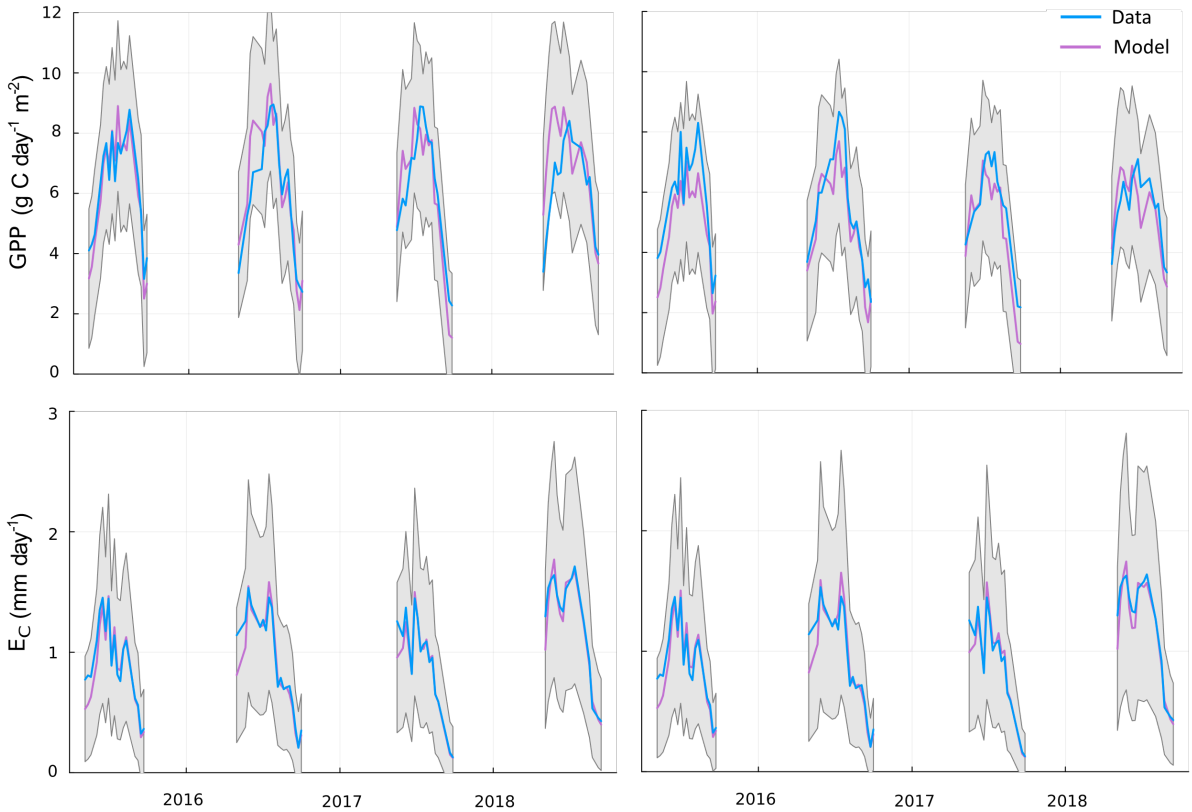

Fig. 3. Result from the parameter estimation case when most of the parameters are shared between the two sand treatments, fertilized stand (fist column) and control (second column). The first and second row depicts the data against the corresponding simulated estimated values for ecosystem gross primary production (GPP) and canopy transpiration (E_C), respectively. The purple lines are the simulated data and the blue lines are the corresponding datapoints. The 95% confidence interval of the model prediction is depicted by the light grey area.

Table 4. Model Performance measure (root-mean-square error, RMSE; Mean absolute percentage error, MAPE; Coefficient of determination R^2) during the parameter estimation (training) and model validation (validation). Parameters where shared among both stand treatments (fertilized and control). Note, the RMSE, MAPE, and R^2 values are calculated as the averages over 10 parameter estimation runs and R^2 was calculated over all datapoints (training + validation).

	GPP		E_C	
	Training	**Validation**	**Training**	**Validation**
		Fertilized		
RMSE	1.10 g C m^{-2} ground day^{-1}	1.03 g C m^{-2} ground day^{-1}	0.11 mm day^{-1}	0.10 mm day^{-1}
MAPE	15.91 %	14.26 %	7.39 %	6.89 %
R^2	0.6		0.93	
		Control		
RMSE	0.82 g C m^{-2} ground day^{-1}	0.86 g C m^{-2} ground day^{-1}	0.11 mm day^{-1}	0.10 mm day^{-1}
MAPE	13.86 %	13.74 %	8.04 %	7.76%
R^2	0.71		0.93	

The model can capture the differences between fertilized and control stands based on only two parameters: the root-canopy hydraulic conductance per leaf area, $k_{rc,\max}$, and the site-specific nitrogen cost parameter, N_s

The summary statistics of the shared and non-shared parameter estimation case showed similar predictive performance. For the non-shared parameter case the average R^2 was 0.68 (GPP) and 0.93 (E_C) for F and 0.75 (GPP) and 0.93 (E_C). See *Methods* S5 and Table S2 for the full list of results. The result suggests that the difference between the two treatments can be well captured by the difference in parameters of soil N availability (N_s) and hydraulic conductivity per leaf area ($k_{rc,\max}$). N_s (unit less) was 0.023 and 0.051 and $k_{rc,\max}$ was 0.94 mmol m^{-2} leaf s^{-1} MPa^{-1} and 1.3 mmol m^{-2} leaf s^{-1} MPa^{-1} for the fertilized and control treatments, respectively (Table 3).

Environmental drivers of leaf N concentration, stomatal conductance, and water use efficiency

Fig. 4 illustrates the variation in optimal traits stomatal conductance ($g_{s,\mathrm{top}}$) and leaf N concentration ($N_{m,f,\mathrm{top}}$) with respect to the weather variables irradiance (I_0), mean ambient temperature (T_a), vapor pressure deficit (VPD), and soil water content (θ). We calculated the correlation (Pearson) between the traits and the weather variables. For $N_{m,f}$ the correlation was 0.35, -0.61, -0.02, and 0.23 for I_0, T_a, VPD, and θ, respectively. For g_s the corresponding values were -0.74, -0.33, -0.87, 0.35. The result indicates that the optimal value of $N_{m,f}$ mostly respond to changes in T_a. g_s on the other hand, responds mostly to the change in VPD and I_0. Correlation values shown here are for the fertilized stand. The control showed similar results and these values can be viewed in Table S3.

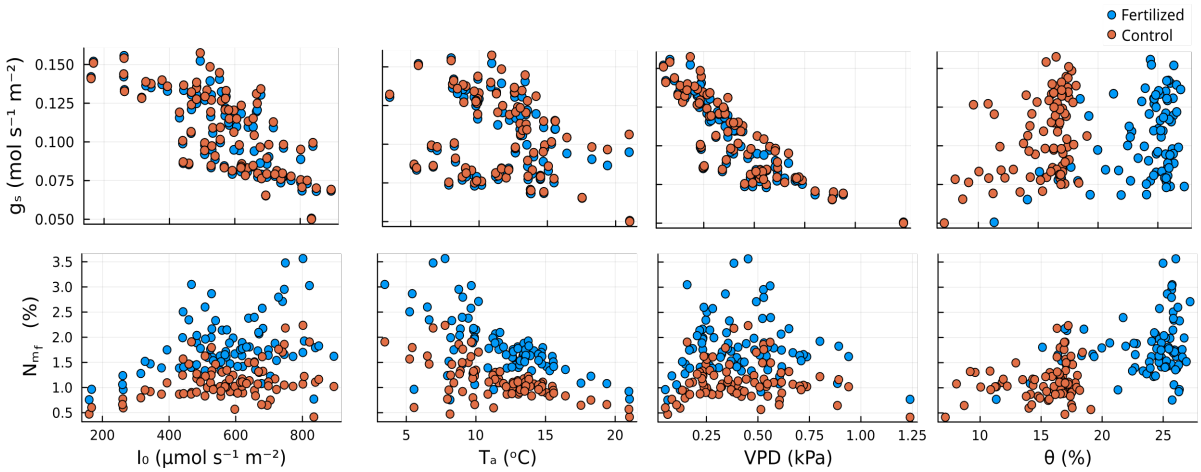

Fig. 4. Response of the optimal traits, stomatal conductance (g_s, first row) and leaf mass-based N concentration ($N_{m,f}$, second row) to change in weather variables: above canopy photosynthetic active radiance (I_0, first column), mean ambient air temperature (T_a, second column), vapor pressure deficit (VPD, third column), and soil water content (θ, fourth column). The blue circles correspond to the optimal trait values for the fertilized stand (F) and orange circles correspond to the control stand (C). The figure was generated by applying the model to the environmental data (Fig. 2), using parameters from Table 2 and Table 3 (case 1, treatment F and C).

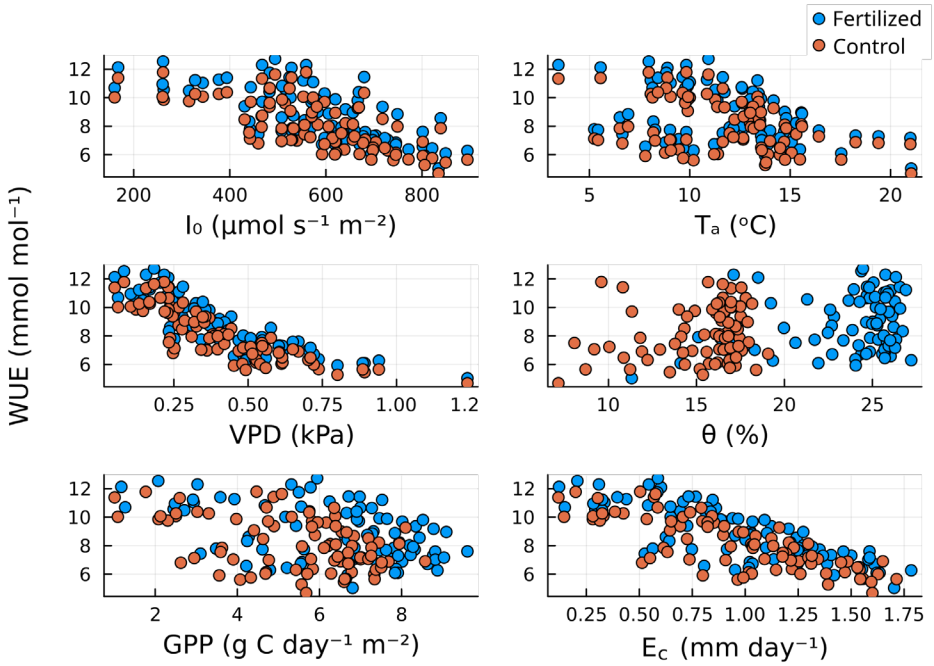

Fig. 5. Water use efficiency responds to change in weather variables: above canopy photosynthetic active radiance (I_0), mean ambient air temperature (T_a), vapor pressure deficit (VPD), soil water content (θ), and gross primary production (GPP) and canopy transpiration (E_C). The blue circles correspond to the optimal trait values for the fertilized stand (F) and orange circles correspond to the control stand (C). The figure was generated by applying the model to the environmental data (Fig. 2), using parameters from Table 2 and Table 3 (case 1, treatment F and C).

The response of water use efficiency, $\mathrm{wue} = A_{\mathrm{top}}/E_{\mathrm{top}}$, to weather data I_0,T_a, VPD, and θ are shown in Fig. 5; here, $E_{\mathrm{top}} = 1.6 g_{s,\mathrm{top}} VPD/P$. The correlation (Pearson) between wue and weather variables was -0.69, -0.41, -0.85, 0.25 for I_0, T_a, VPD, and θ, respectively. From the correlation values and Fig. 5 we see that wue responds similarly to the various weather variables as g_s. In contrast, the wue response showed little resemblance to the weather response of $N_{m,f,\mathrm{top}}$, indicating that wue is mainly influenced by $g_{s,\mathrm{top}}$. This is also supported by the fact that wue is more strongly linked to canopy transpiration than GPP (Fig. 5).

The fertilization treatment led to reduced stomatal conductance and increased leaf N concentration (Fig. 4), which resulted in higher WUE. The fertilized plots also had a substantially higher soil water content than the control plots (Tian *et al.*, 2021).

Discussion

Model scope and limitations

Our model estimates canopy transpiration (E_c) and GPP, based on optimal acclimation of stomatal conductance and leaf nitrogen (N) concentration. The model can for the most part accurately predict observed inter- and intra-seasonal variation of E_c and GPP at the two study stands (Fig. 3). An exception is the growth period of 2018, where the site was hit by a severe drought period. In this period the model overestimates GPP for both the fertilized stand and the control (Fig. S1). This divergence can probably be linked to the fact that we use a fixed potential hydraulic conductivity, i.e. not accounting for hydraulic damages, see below. Our results demonstrate that the effect of fertilization, can be captured by changes in only two parameters: the root-canopy hydraulic conductance per leaf area, $k_{rc,\max}$, and the site-specific N cost parameter, N_s.

The current version of the model predicts GPP and transpiration for trees with a given LAI and potential hydraulic conductivity per LAI ($k_{rc,\max}$). As such, it is naturally unable to predict dynamics in these properties, which could be addressed in future versions of the model (see Conclusions and Outlook, below).

Another dynamic limitation of the current model version is that we used weekly mean values for input variables and consequently the optimized trait values are also weekly mean values. This temporal resolution was used to match the expected response time of leaf N ($N_{m,f}$). Real acclimation of stomatal conductance ($g_{s,\mathrm{top}}$) is faster and regulates on a sub daily timescale. For future improvement, a hierarchical optimization method could be implemented to optimize leaf N and stomatal conductance on different timescales.

The impact of increased soil N concentration.

The difference between our model and the previous models by Eller et al. (2018) and Prentice et al. (2014) is that we do not only account for optimal stomatal response but also optimize leaf N concentration. Another recent model that also allows optimization of stomatal conductance and $J_{\max}$, which is functionally equivalent to our optimization of leaf N, is the model by Joshi et al. (2022). However, this model has a different hydraulic cost function and, more importantly, does not address variation in the cost of N uptake related to soil N availability.

Our model allows us to account for the response to increased soil N availability. In agreement with our model predictions, it has been observed that increased soil N availability results in increased leaf N concentration (Inselsbacher *et al.*, 2014; Lim *et al.*, 2015) . This in turn has a positive impact on the potential photosynthetic capacity and the $J_{\max}$ in our model. The model results further implies that increased soil N availability decreases C cost of N uptake (the cost parameter N_s). This reduction means that the trees must invest less C to maintain a given leaf N concentration and consequently a given potential photosynthetic capacity. It should be noted that if we assume a constant $N_{m,f}$ our model would converge to the general framework of the SOX model. Beside the decrease in N_s we also get a decrease in estimated conductivity per leaf area ($k_{rc,\max}$) in the fertilized plot. $k_{rc,\max}$ was 28% larger for the control than the fertilized plot. This is partially due to the observed higher LAI in the fertilized plot, corresponding to an approximately 12% lower Huber value (sapwood area / leaf area), in the fertilized compared with the control stand (calculated from field measurements).

The responses of leaf variables and water use efficiency to weather variables

Based on our results we can infer that the optimal leaf N concentration ($N_{m,f,\mathrm{top}}$) is negatively correlated with temperature (Fig. 4). This is in line with empirical observations for Scots pine (Zha et al. 2002), understory evergreen species (Muller *et al.*, 2011) and a global biogeographic pattern of different plant species (Reich & Oleksyn, 2004). This is caused by the shape of the C assimilation curve and the cost of maintaining $J_{\max}$ as functions of $N_{m,f}$. The optimum $N_{m,f}$ will occur when the slope of the C assimilation function is equal to the slope of the cost line. When the temperature increases the slope of the cost line increases more than the C assimilation curve, thus the optimal $N_{m,f}$ will decrease. This temperature effect further implies that the leaf nitrogen content should decrease with high temperatures in the middle of the growth season (Fig. S7). Because the model only accounts for photosynthetic N but not other N that may respond differently, it probably overestimates the seasonal variation in N. Nevertheless, qualitatively similar seasonal variation has been observed in other Scots pine stands (Wyka et al. 2016).

Unsurprisingly, we found that stomatal $g_{s,\mathrm{top}}$ correlated best with VPD. A high VPD leads to an increase in water loss for fixed value of g_s, thus $g_{s,\mathrm{top}}$ is negatively correlated to VPD to reduce cost for maintaining transpiration. Surprisingly however, our results (Fig. 4) appear to suggest that the

stomatal $g_{s,\mathrm{top}}$ is negatively correlated to the above canopy photosynthetic active radiance (I_0). However, this is only the result of confounding variation in other drivers, as concluded by running the model with fixed weather variables except for I_0. Furthermore, we found that the response of wue to the environmental variables closely follows that of $g_{s,\mathrm{top}}$ (Fig. 5). Thus, wue is more strongly correlated to $g_{s,\mathrm{top}}$ than $N_{m,f,\mathrm{top}}$. This is not surprising as the transpiration is directly determined by $g_{s,\mathrm{top}}$ and wue varies highly with E_C. In all cases, soil water content (θ) had a small impact on $g_{s,\mathrm{top}}$, $N_{m,f,\mathrm{top}}$, and wue when θ is large (approximately $\theta > 20\%$ for F treatment and $\theta > 15\%$ for C treatment). For low soil water content, a decrease in θ leads to decreases in $g_{s,\mathrm{top}}$, $N_{m,f,\mathrm{top}}$, and wue, driving the observed positive correlation between θ and the plant variables and process rates. The difference between high and low θ is caused by the monotonically decreasing concave down shape of the vulnerability function, $P(\psi)$. For low values of θ (highly negative soil water potential, ψ_s), the increase in cost associated with small change in trait values (the derivative of the cost with respect to the traits) is larger than for higher θ.

While $g_{s,\mathrm{top}}$, $N_{m,f,\mathrm{top}}$ both correlate well with different weather variables, there is only a weak negative correlation between the two traits (Pearson correlation = -0.25 for F treatment and -0.26 for C treatment, see Fig. S6). This implies that $g_{s,\mathrm{top}}$ and $N_{m,f,\mathrm{top}}$ mostly responds to different weather variables. $g_{s,\mathrm{top}}$ responds strongly to irradiance and VPD, while $N_{m,f,\mathrm{top}}$ responds strongly to the ambient temperature.

Conclusions and outlook

The key scientific advancement made by this model lies in its ability to explain and accurately predict the interacting effects of climate, soil water, and soil N availability on GPP and transpiration, based on an eco-evolutionary optimality principle (EEO). This capacity makes the model well suited for studying the impact of climate change in N limited forests, and effects of changes in soil N availability such as fertilization treatments and N deposition. However, one has to be careful when applying the model to severe drought conditions as it does not yet account for accumulation of hydraulic damages. To address longer term effects and forest growth, the model can be extended with the capacity to predict carbon allocation to the different plant organs, such as branches, fine root, stem, and leaves. To this end, our model could be coupled with allocation models based on similar EEO principles (e.g., Franklin et al., 2012 and Fransson et al., 2021).

Acknowledgement

The work presented in this paper was funded by the Knut and Alice Wallenberg Foundation (Grant 2018.0259).

Author contributions

All authors discussed the results and implications and revised the manuscript. O.F. and P.F conceived the study and formulated the model. P.F. implemented and analyzed the model, and wrote the first draft of the manuscript. H.L. and P.Z. provided data and data analysis.

References

Alduchov OA, Eskridge RE. **1996**. Improved Magnus Form Approximation of Saturation Vapor Pressure. *Journal of Applied Meteorology* **35**: 601–609.

Ball JT, Woodrow IE, Berry JA. **1987**. A Model Predicting Stomatal Conductance and its Contribution to the Control of Photosynthesis under Different Environmental Conditions. In: Progress in Photosynthesis Research.

Binkley D, Högberg P. **2016**. Tamm Review: Revisiting the influence of nitrogen deposition on Swedish forests. *Forest Ecology and Management* **368**: 222–239.
Chen JL, Reynolds JF, Harley PC, Tenhunen JD. **1993**. Coordination theory of leaf nitrogen distribution in a canopy. *Oecologia* **93**: 63–69.
Chi J, Zhao P, Klosterhalfen A, Jocher G, Kljun N, Nilsson MB, Peichl M. **2021**. Forest floor fluxes drive differences in the carbon balance of contrasting boreal forest stands. *Agricultural and Forest Meteorology* **306**.
Cowan IR, Farquhar GD. **1977**. Stomatal function in relation to leaf metabolism and environment. *Symposia of the Society for Experimental Biology* **31**.
Eller CB, Rowland L, Oliveira RS, Bittencourt PRL, Barros F V., Da Costa ACL, Meir P, Friend AD, Mencuccini M, Sitch S, *et al.* 2018. Modelling tropical forest responses to drought and El Niño with a stomatal optimization model based on xylem hydraulics. *Philosophical Transactions of the Royal Society B: Biological Sciences* **373**.
Farquhar GD, von Caemmerer S. **1982**. Modelling of Photosynthetic Response to Environmental Conditions. In: Physiological Plant Ecology II.
Farquhar GD, von Caemmerer S, Berry JA. **1980**. A biochemical model of photosynthetic CO2 assimilation in leaves of C3 species. *Planta* **149**: 78–90.
Feldt R. **2018**. BlackBoxOptim.jl. *GitHub repository*.
Franklin O. **2007**. Optimal nitrogen allocation controls tree responses to elevated CO 2. *New Phytologist* **174**: 811–822.
Franklin O, Johansson J, Dewar RC, Dieckmann U, McMurtrie RE, Brännström Å, Dybzinski R. **2012**. Modeling carbon allocation in trees: A search for principles. *Tree Physiology* **32**: 648–666.
Fransson P, Brännström Å, Franklin O. **2021**. A tree's quest for light-optimal height and diameter growth under a shading canopy. *Tree Physiology* **41**: 1–11.
Hari P, Mäkelä A. **2003**. Annual pattern of photosynthesis in Scots pine in the boreal zone. *Tree Physiology* **23**: 145–155.
Inselsbacher E, Oyewole OA, Näsholm T. **2014**. Early season dynamics of soil nitrogen fluxes in fertilized and unfertilized boreal forests. *Soil Biology and Biochemistry* **74**: 167–176.
IPCC. **2014**. IPCC Fifth Assessment Synthesis Report-Climate Change 2014 Synthesis Report. *IPCC Fifth Assessment Synthesis Report-Climate Change 2014 Synthesis Report*.
Jansson P-E, Karlberg L. **2011**. *Coupled Heat and Mass Transfer Model for Soil-Plant-Atmosphere Systems*. Stockholm, Sweden.
Jenkins A. **2013**. The Sun's position in the sky. *European Journal of Physics* **34**: 633–652.
Joshi J, Stocker BD, Hofhansl F, Zhou S, Dieckmann U, Prentice IC. **2022**. Towards a unified theory of plant photosynthesis and hydraulics. *Nature Plants* **8**: 1304–1316.
K Mogensen P, N Riseth A. **2018**. Optim: A mathematical optimization package for Julia. *Journal of Open Source Software* **3**: 615.
Landsberg JJ, Sands P. **2010**. *Physiological ecology of forest production: principles, processes and models*. Academic Press.
Lim H, Oren R, Palmroth S, Tor-ngern P, Mörling T, Näsholm T, Lundmark T, Helmisaari HS, Leppälammi-Kujansuu J, Linder S. **2015**. Inter-annual variability of precipitation constrains the production response of boreal Pinus sylvestris to nitrogen fertilization. *Forest Ecology and Management* **348**: 31–45.
Mäkelä A, Hari P, Berninger F, Hänninen H, Nikinmaa E. **2004**. Acclimation of photosynthetic capacity in Scots pine to the annual cycle of temperature. *Tree Physiology* **24**: 369–376.
Mäkelä A, Pulkkinen M, Kolari P, Lagergren F, Berbigier P, Lindroth A, Loustau D, Nikinmaa E, Vesala T, Hari P. **2008**. Developing an empirical model of stand GPP with the LUE approach: Analysis of eddy covariance data at five contrasting conifer sites in Europe. *Global Change Biology* **14**: 92–108.
Muller O, Hirose T, Werger MJA, Hikosaka K. **2011**. Optimal use of leaf nitrogen explains seasonal changes in leaf nitrogen content of an understorey evergreen shrub. *Annals of Botany* **108**: 529–536.

Näslund M. **1947**. Empirical formulae and tables for determining the volume of standing trees: Scots pine, Norway spruce and birch in southern Sweden and in the whole of the country. *Meddelanden Fran Statens Skogsforskningsinstitut, 36, 81. (in Swedish)*.
Prentice IC, Dong N, Gleason SM, Maire V, Wright IJ. **2014**. Balancing the costs of carbon gain and water transport: Testing a new theoretical framework for plant functional ecology. *Ecology Letters* **17**: 82–91.
Reich PB, Oleksyn J. **2004**. *Global patterns of plant leaf N and P in relation to temperature and latitude*.
Ryan MG. **2011**. Tree responses to drought. *Tree Physiology* **31**: 237–239.
Sage RF, Kubien DS. **2007**. The temperature response of C(3) and C(4) photosynthesis. *Plant, cell & environment* **30**: 1086–106.
Tamm CO. **1991**. *Nitrogen in terrestrial ecosystems: questions of productivity, vegetational changes, and ecosystem stability*. Berlin: Springer Science & Business Media.
Tarvainen L, Lutz M, Räntfors M, Näsholm T, Wallin G. **2018**. Temperature responses of photosynthetic capacity parameters were not affected by foliar nitrogen content in mature Pinus sylvestris. *Physiologia Plantarum* **162**: 370–378.
Tian X, Minunno F, Schiestl-Aalto P, Chi J, Zhao P, Peichl M, Marshall J, Näsholm T, Lim H, Peltoniemi M, *et al.* 2021. Disaggregating the effects of nitrogen addition on gross primary production in a boreal Scots pine forest. *Agricultural and Forest Meteorology* **301–302**.
Tor-Ngern P, Oren R, Oishi AC, Uebelherr JM, Palmroth S, Tarvainen L, Ottosson-Löfvenius M, Linder S, Domec JC, Näsholm T. **2017**. Ecophysiological variation of transpiration of pine forests: Synthesis of new and published results: Synthesis. *Ecological Applications* **27**: 118–133.
Wang H, Prentice IC, Keenan TF, Davis TW, Wright IJ, Cornwell WK, Evans BJ, Peng C. **2017**. Towards a universal model for carbon dioxide uptake by plants. *Nature Plants* **3**: 734–741.
Wolf A, Anderegg WRL, Pacala SW. **2016**. Optimal stomatal behavior with competition for water and risk of hydraulic impairment. *Proceedings of the National Academy of Sciences of the United States of America* **113**: E7222–E7230.
Wyka TP, Żytkowiak R, Oleksyn J. 2016. Seasonal dynamics of nitrogen level and gas exchange in different cohorts of Scots pine needles: a conflict between nitrogen mobilization and photosynthesis? *European Journal of Forest Research* **135**: 483–493
Zha T, Wang K-Y, Ryyppö A, Kellomäki S. 2002. Needle dark respiration in relation to within-crown position in Scots pine trees grown in long-term elevation of CO2 concentration and temperature. *New Phytologist* **156**: 33-41
Zhao P, Chi J, Nilsson MB, Löfvenius MO, Högberg P, Jocher G, Lim H, Mäkelä A, Marshall J, Ratcliffe J, *et al.* 2022. Long-term nitrogen addition raises the annual carbon sink of a boreal forest to a new steady-state. *Agricultural and Forest Meteorology* **324**: 109112.

Supporting Information

Supporting information

Additional supporting information may be found in the online version of this article.

Methods S1. Details regarding the computation of the hydraulic model.
Methods S2. Deriving an expression for the maximum transpiration and integration of the v curve.
Methods S3. Describing how to upscale GPP and E_C values from leaf-level to stand-level.
Methods S4. Description of how to estimate the contribution of understory vegetation to ecosystem GPP.
Methods S5. Result from the parameter estimation case when no shared parameters between the stands.

Fig. S1. Model residuals against the corresponding datapoints for the parameter estimation case when parameters are shared among the fertilized stand and control stand.
Fig. S2. Statistical summaries of the result from parameter estimation for the parameter estimation case when parameters are shared among for the fertilized stand and control stand.
Fig. S3. Model estimates of GPP and E_C, from the parameter estimation case when no parameters are shared between the fertilized stand and control, against data.
Fig. S4. Statistical summaries of the result from parameter estimation for the parameter estimation case when no parameters are shared among for the fertilized stand and control stand.
Fig. S5. Model residuals against the corresponding datapoints for the parameter estimation case when no parameters are shared among the fertilized stand and control stand.
Fig. S6. Optimal stomatal conductance (g_s) against optimal leaf mass-based N concentration ($N_{m,f}$).
Fig. S7. Optimal stomatal conductance (g_s) and optimal leaf mass-based N concentration ($N_{m,f}$). against time.
Table S1. Canopy GPP scaling factor and the fraction contribution of ground vegetation layer to eco system GPP.
Table S2. Estimated parameter values for the case when no parameters are shared between the two stand treatments.
Table S3. Pearson correlation between model outputs and weather variables.